J Biomol NMR (2011) 51:313–318
DOI 10.1007/s10858-011-9572-7

ARTICLE

4D APSY-HBCB(CG)CDHD experiment for automated assignment of aromatic amino acid side chains in proteins

Barbara Krähenbühl · Sebastian Hiller · Gerhard Wider

Received: 27 May 2011 / Accepted: 6 August 2011 / Published online: 27 September 2011

Abstract A four-dimensional (4D) APSY (automated projection spectroscopy)-HBCB(CG)CDHD experiment is presented. This 4D experiment correlates aromatic with aliphatic carbon and proton resonances from the same amino acid side chain of proteins in aqueous solution. It thus allows unambiguous sequence-specific assignment of aromatic amino acid ring signals based on backbone assignments. Compared to conventional 2D approaches, the inclusion of evolution periods on $^{1}H^{\beta}$ and $^{13}C^{\delta}$ efficiently removes overlaps, and provides two additional frequencies for consequent automated or manual matching. The experiment was successfully applied to three proteins with molecular weights from 6 to 13 kDa. For the complementation of the assignment of the aromatic resonances, TOCSY- or COSY-based versions of a 4D APSY-HCCH^{aro} sequence are proposed.

Keywords Protein NMR · Aromatic resonances · Projection spectroscopy · APSY · GAPRO · Automated assignment

Electronic supplementary material The online version of this article (doi:10.1007/s10858-011-9572-7) contains supplementary material, which is available to authorized users.

B. Krähenbühl · G. Wider (✉)
Institute of Molecular Biology and Biophysics, ETH Zurich, 8093 Zurich, Switzerland
e-mail: gsw@mol.biol.ethz.ch

S. Hiller
Biozentrum, University of Basel, 4056 Basel, Switzerland

Introduction

Aromatic amino acids are often involved in the hydrophobic core of proteins, or play a role in their active sites. Hence, detailed structural and functional analysis of proteins by NMR depends on the sequence-specific assignment of the aromatic NMR signals. This requires the correlation of the aromatic resonances to signals included in the backbone assignment. A common way for simple cases is the correlation of ring protons to $^{1}H^{\alpha}$ and $^{1}H^{\beta}$ by through-space NOE experiments (Billeter et al. 1982; Wagner and Wüthrich 1982). The first experiments which provided unambiguous correlations in ^{13}C-labeled proteins by through-bond transfers were the (HB)CB(CGCD)HD and (HB)CB(CGCDCE)HE experiments (Yamazaki et al. 1993). Different modifications of these 2D experiments have been developed, which replaced COSY-type transfer between carbons by TOCSY transfer elements (Carlomagno et al. 1996; Grzesiek and Bax 1995; Löhr et al. 2007; Zerbe et al. 1996). Other strategies to achieve backbone-to-ring correlations are a set of 'out-and-back' TROSY experiments, which are then matched on $^{13}C^{\gamma}$ (Löhr et al. 2002), or experiments based on long-range scalar couplings with regioselectively labeled proteins (Torizawa et al. 2005). A detailed comparison and discussion of aromatic side chain experiments was recently published (Löhr et al. 2007).

The development of reduced dimensionality spectroscopy methods (Szyperski et al. 1993, 2002; Kupce and Freeman 2003) has opened new perspectives also for the assignment of aromatic side chains. Among them, automated projection spectroscopy (APSY) has proven successful for protein backbone and non-aromatic side chain assignments (Fiorito et al. 2006; Gossert et al. 2007, 2011; Hiller et al. 2005, 2007, 2008a, b). In APSY, peak lists

from a series of 2D projection spectra (Kupce and Freeman 2003) provide the input for the algorithm GAPRO (Hiller et al. 2005) which calculates geometrically a precise multidimensional chemical shift correlation list. The main advantages of APSY experiments are their robustness in delivering precise high-dimensional peak lists, and the high spectral resolution due to the high dimensionality that reduces overlap problems. Overall, APSY peak lists form a reliable basis for sequence-specific resonance assignments.

Here, a new 4D APSY-HBCB(CG)CDHD experiment is presented. It is applicable to all four natural aromatic amino acids simultaneously (His, Phe, Trp, Tyr), and does not require regioselective isotope labeling. Compared to the conventional 2D and 3D approaches, the inclusion of 1–2 additional dimensions yields unambiguous connectivities of the aromatic ring systems to the assigned protein backbone by matching $^{1}H^{\beta}$ and $^{13}C^{\beta}$ chemical shifts. As a possible complementary experiment for the assignment of the remaining aromatic resonances, a 4D APSY-HCCH-TOCSY derived from a 3D HCcH-TOCSY sequence (Bax et al. 1990) is proposed.

Materials and methods

Sample preparation

The three different proteins (GB1, ubiquitin, and TM1290) used in this work were [*U*-^{13}C, ^{15}N]-labeled. The expression and purification protocol of GB1 was described previously (Takeuchi et al. 2010; Früh et al. 2005). GB1 had a protein concentration of 1 mM for a sample volume of ~280 µl in a Shigemi microcell (Shigemi Inc, Allison Park, PA, USA), and contained 10 mM phosphate buffer at pH 6.0, 5% D_2O and 0.02% NaN_3. Ubiquitin was obtained as described previously (Burschowsky et al. 2011). The NMR sample had a final protein concentration of 3.8 mM in 25 mM phosphate buffer at pH 6.0, and contained 5% D_2O and 0.02% NaN_3. TM1290 was produced as described previously (Etezady-Esfarjani et al. 2003; Etezady-Esfarjani et al. 2004). The sample had a concentration of 1 mM, and contained 20 mM phosphate buffer at pH 6.0, 0.05% NaN_3 and 5% D_2O. The protein concentrations were determined using the method PULCON (Wider and Dreier 2006).

Description of the pulse sequence

The magnetization transfer pathway of the 4D APSY-HBCB(CG)CDHD experiment is illustrated for phenylalanine in Fig. 1, the corresponding pulse sequence in Fig. 2. The experiment starts with the β-protons and detects the signal on the δ-protons (partially also on the ε-protons; see below) after being transferred via C^{β}, C^{γ} and C^{δ} (Fig. 1).

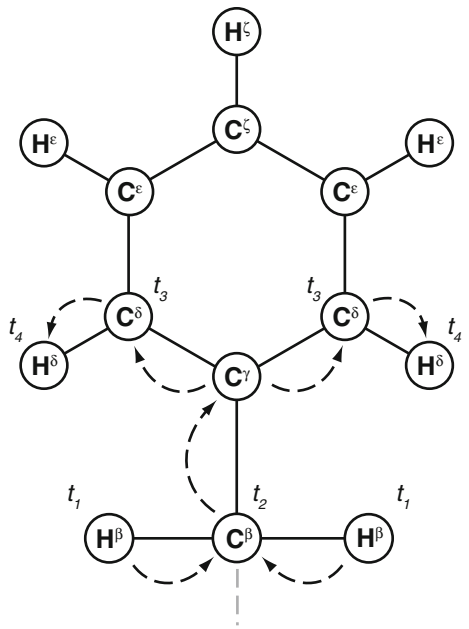

Fig. 1 Magnetization transfer pathway in the 4D APSY-HBCB(CG)CDHD experiment. Coherence transfer steps via scalar couplings are indicated by *dashed arrows*. The overall pathway corresponds to the original 2D (HB)CB(CGCD)HD experiment (Yamazaki et al. 1993), but two additional evolution periods for frequency labeling were introduced. The resulting three indirect evolution periods are indicated by t_1–t_3 and the acquisition time by t_4. In addition to the evolution of $^{13}C^{\beta}$ magnetization during t_2, the magnetization on $^{1}H^{\beta}$ and $^{13}C^{\delta}$ evolve during t_1 and t_3, respectively

Compared to the 2D experiment by Yamazaki and coworkers (Yamazaki et al. 1993), two additional evolution periods, namely for β-protons ($^{1}H^{\beta}$) and δ-carbons ($^{13}C^{\delta}$) have now been added, resulting in a 4D scheme. For the first new evolution period, the initial INEPT (Morris and Freeman 1979) element connecting the β-protons and β-carbons ($^{13}C^{\beta}$) is modified to include a semi-constant time evolution (Grzesiek and Bax 1993; Logan et al. 1993) for the $^{1}H^{\beta}$. The constant time evolution on δ-carbons is included into the inverse INEPT step during the time period T_3. Since the optimal T_3 values are short for an evolution time, the $^{13}C^{\delta}$–$^{13}C^{\gamma}$ transfer period is prolonged here from 4.2 ms [suggested by Yamazaki et al. (1993)] to 5.2 ms in order to allow higher resolution in the $^{13}C^{\delta}$ dimension. Longer T_3 favor coherence transfer in histidine (His) and tryptophan (Trp) relative to phenylalanine (Phe) and tyrosine (Tyr). In case the sensitivity on Phe and Tyr becomes limiting in a particular application, the resolution in the $^{13}C^{\delta}$ dimension can be reduced.

Data acquisition and processing

Experiments were performed on Bruker Avance III spectrometers with proton Larmor frequencies of 500, 700 and 750 MHz equipped with triple resonance $^{1}H/^{13}C/^{15}N$

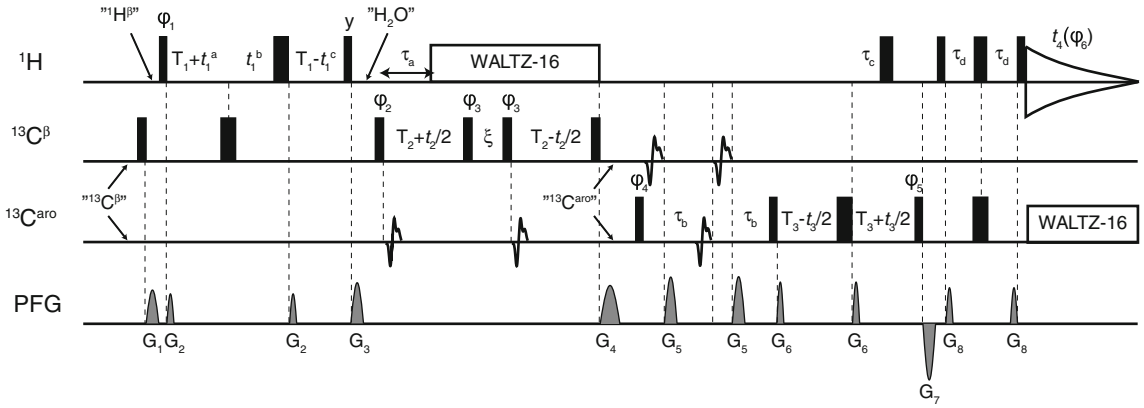

Fig. 2 Pulse sequence of the 4D APSY-HBCB(CG)CDHD experiment. The carrier frequency for protons during the first INEPT element was set in the β-proton region at 2.85 ppm, indicated on the line ^{1}H by "$^{1}H^{\beta}$"; at the position "H_2O" the carrier was set to the water frequency. Native ^{13}C magnetization is suppressed with a 90° pulse and a subsequent gradient (G_1) prior to the first INEPT. Water is suppressed by gradients, if necessary suppression can be improvement by presaturation during the recycle delay. Radio-frequency pulses on carbons at the beginning of the sequence were applied at 36.5 ppm for β-carbons, indicated by "$^{13}C^{\beta}$" and the carrier frequency was moved to 127 ppm for aromatic carbons at the position "$^{13}C^{aro}$". Thin and wide rectangular bars represent 90° and 180° high-power pulses. For ^{13}C, the durations of rectangular 90° pulses are adjusted to $\sqrt{15/(4\Delta)}$, with Δ being the frequency difference between $^{13}C^{aro}$ and $^{13}C^{\beta}$ in order not to excite $^{13}C^{aro}$ with $^{13}C^{\beta}$ pulses and vice versa. For selective inversion of $^{13}C^{\beta}$ or $^{13}C^{aro}$, Q3 Gaussian cascades (Emsley and Bodenhausen 1990) (*shapes* on the lines $^{13}C^{\beta}$ and $^{13}C^{aro}$) are applied with durations of 250 µs on $^{13}C^{aro}$ and 350 µs on $^{13}C^{\beta}$ on a 700 MHz spectrometer. WALTZ-16 (Shaka et al. 1983) decoupling sequences (*white rectangles*) were applied on ^{1}H during t_2 evolution and on $^{13}C^{aro}$ during acquisition. $\xi = 1/(2\Delta) - (4/\pi)\tau_{90}$ (see Yamazaki et al. 1993), where Δ is the offset difference $^{13}C^{\alpha}/^{13}C^{\beta}$, and τ_{90} the 90° ^{13}C pulse length. The initial delays in the evolution periods are $T_1 = 1.7$ ms, $T_2 = 2.6$ ms, and $T_3 = 2.6$ ms. Further time periods are $\tau_a = 1.8$ ms, $\tau_b = 2.7$ ms, $\tau_c = 1.21$ ms, and $\tau_d = 1.25$ ms. The pulse phases were set to x unless indicated otherwise above the pulse symbol. The following phase cycle was used: $\varphi_3 = x, y, -x, -y$; $\varphi_4 = 4(x), 4(y)$; $\varphi_6 = 2(x, -x), 2(-x, x)$ (receiver phase). The incremented phases and delays to achieve States-TPPI quadrature detection (Marion et al. 1989) for the indirect dimensions are φ_1 for $t_1(^{1}H^{\beta})$, φ_2 for $t_2(^{13}C^{\beta})$, and φ_5 for $t_3(^{13}C^{\delta})$. $^{1}H^{\beta}$ evolution was achieved in a constant time manner with $t_1^a = t_1/2$, $t_1^b = t_1^a - t_1^c$ and $t_1^c = T_1/\mathrm{TD}$ with TD = number of increments. The sine-bell shaped gradient pulses were applied with the following durations and strengths: G_1: 1,000 µs, 10 G/cm; G_2: 500 µs, 7.5 G/cm; G_3: 1,000 µs, 15 G/cm; G_4: 2,000 µs, 16 G/cm; G_5: 1,000 µs, 20 G/cm; G_6: 450 µs, 12.5 G/cm; G_7: 1,000 µs, −30 G/cm; G_8: 500 µs, 8.5 G/cm

probes with z-gradient accessory. The 750 MHz spectrometer is operated with a conventional room temperature probe, the two other instruments with cryogenic probes. The projection experiments were set up from a parent data set with a macro script ("AU" program) using the spectrometer software Topspin 2.1 (Bruker, Karlsruhe, Germany). Automated serial processing with automatically generated input files was performed with Prosa 6.4 (Güntert et al. 1992). The subsequent peak picking in the projection spectra, and the calculation of the multidimensional peak lists were performed by GAPRO 0.98 (Hiller et al. 2005). A more detailed description of the procedure to measure and analyze the experiments is provided in the Supplementary Material.

Automated assignment strategies

The backbone assignments for the three proteins were obtained from the Biological Magnetic Resonance Data Bank (BMRB, http://www.bmrb.wisc.edu). Possible differences in the chemical shift calibration were minimized by a least square fit to a set of clearly corresponding β-proton and β-carbon resonances. The connection of the APSY 4D peak list to the backbone assignment was obtained using a software routine programmed in MATLAB (R2010b, The MathWorks, Natick, MA, USA). The script reads the required data from the sequential backbone assignment in NMR-STAR format obtained from the BMRB, matches the 4D peaks of the 4D APSY-HBCB(CG)CDHD to the nearest chemical shifts of the nuclei $^{13}C^{\beta}$, $^{1}H^{\beta 2}$ and $^{1}H^{\beta 3}$ from the backbone assignment, and creates a list with the sequence specific assignment of the aromatic resonances. The script can optionally visualize the matching procedure in a plot (see "Results and discussion", and Fig. S1 in the Supplementary Material). For the assignment of the remaining aromatic resonances (ε, ζ and η protons and carbons), a MATLAB script with the same features can subsequently be executed, which matches the 4D aromatic ring peak list from a 4D APSY-HCCH experiment to the previous assignment.

Results and discussion

A 4D APSY-HBCB(CG)CDHD experiment is presented, which allows automated assignment of aromatic carbon and proton resonances. The experiment exploits a magnetization transfer pathway (Fig. 1) commonly used for the

assignment of aromatic side chains in uniformly ^{13}C-labeled proteins (Yamazaki et al. 1993). In the APSY version, three evolution periods are placed along this pathway, resulting in a 4D experiment. The additional dimensions significantly reduce signal overlap and consequential assignment ambiguity. The pulse scheme does not require amino acid-selective labeling, and is applicable to all four proteinogenic aromatic amino acids simultaneously.

The new experiment was developed and tested with ubiquitin and applied to TM1290 and GB1. TM1290 contains six Phe, four Tyr, and one His, but no Trp, neither does ubiquitin (1 Phe, 1 Tyr, 1 His). Therefore, the performance of the experiment for tryptophan was tested with GB1 which contains 3 Phe, 2 Tyr, 1 Trp and, in our preparation, a His_6-tag. For the protein TM1290, a complete peak list containing all β-protons, β-carbons, δ-carbons and δ-protons was obtained from 19 projections that were measured in 13 h at 20°C on a Bruker Avance III 700 MHz spectrometer. The experimental details on projection angles, on the sweep widths, the maximal evolution times and measurement times of individual planes are listed in Tables S1 and S2 in the Supplementary Material. Figure 3 presents the three orthogonal projections with the frequency ranges for δ-carbons, β-carbons and β-protons, respectively, in the indirect dimension versus the chemical shifts of aromatic δ-protons in the acquisition dimension. The dynamic range for the signal intensities of the individual aromatic residues is considerable. Still, even for the weakest signals (β-protons of Phe 21), which barely can be distinguished from thermal noise, GAPRO produces precise chemical shifts (Fig. 3).

For ubiquitin a complete 4D APSY peak list was obtained from 15 projections measured at 20°C in 12.6 h on a Bruker Avance III 750 MHz spectrometer. The detection of Trp was verified in an experiment with 13 projections measured with GB1 at 25°C in 4 h at 750 MHz on a room temperature probe.

The 4D ($^1H^\beta$, $^{13}C^\beta$, $^{13}C^\delta$, $^1H^\delta$)-chemical shift correlations resulting from the 4D APSY-HBCB(CG)CDHD experiments were matched via their $^1H^\beta$ and $^{13}C^\beta$ chemical shifts to the backbone assignment with MATLAB scripts (see "Materials and methods"). The 4D peak list of TM1290 could be completely and unambiguously matched for all residues for which $^1H^\beta$ and $^{13}C^\beta$ chemical shifts were contained in the backbone assignment (Etezady-Esfarjani et al. 2003) therein. This was the case for all Phe and Tyr residues; only the β-CH_2 group of His 48 was missing. The 4D APSY peak list contained two chemical shift correlations, which clearly corresponded to a single His spin system with non-degenerate $^1H^\beta$ chemical shifts. Since only one His is contained in TM1290, it could thus be unambiguously assigned (Fig. 3 and supplementary Fig. S1). In addition to correlations with the δ-protons of the aromatic rings, three weak correlations to ε-protons due to strong coupling effects between the δ- and ε-carbons in the corresponding residues were detected. Two of the 4D peaks could be assigned to $^1H^\varepsilon$ of Phe 101 at 6.38 ppm (Fig. 3), and one to $^1H^\varepsilon$ of Phe 76 at 7.01 ppm. The matching procedure showed that connecting exclusively via the $^{13}C^\beta$ chemical shifts would have been ambiguous for residues Phe 21/Phe 76 and Phe 101/Phe 112, and difficult for residues Phe 27/Tyr 30/Tyr 87 as well as for Phe 89/Tyr 65 (Supplementary Material Fig. S1) without the more precise and higher dimensionality data from APSY. Even though the chemical shift dispersions of both $^{13}C^\beta$ and $^{13}C^\delta$ are rather narrow (but uncorrelated) in Tyr and Phe their combined use does resolve overlap problems.

The 4D peaks derived from the ubiquitin experiment were completely and automatically matched to the previously published backbone assignment (Cornilescu et al. 1998) with the exception of His 68, which was outside the

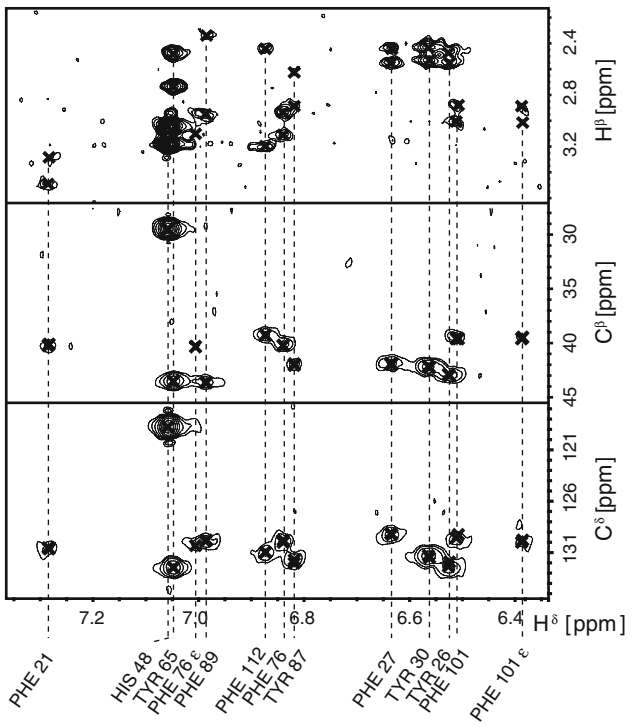

Fig. 3 Three 2D projection spectra from a 4D APSY-HBCB(CG)CDHD experiment with the protein TM1290, representing the $^1H^\beta$–$^1H^\delta$, the $^{13}C^\beta$–$^1H^\delta$ and the $^{13}C^\delta$–$^1H^\delta$ correlations, i.e. the orthogonal projections (α, β) = (0°, 90°) (90°, 0°) and (0°, 0°), respectively. Complete 4D peak lists were obtained from 19 projections of the four-dimensional experiment measured on a 700 MHz spectrometer within 13 h at 20°C. The exact positions of the resonances in the different projections were calculated from the multidimensional APSY peak list; these positions are marked by *black crosses*. *Dashed lines* indicate the chemical shifts of the aromatic δ-protons, $^1H^\delta$, in the acquisition dimension, and are labeled with the three letter amino acid code and the sequence number. The correlations to $^1H^\varepsilon$ are visible for Phe 101 and Phe 76 (details see text)

matching range due to chemical shift deviations because of a different pH of the solutions (Sachs et al. 1971): pH 6.0 in our measurement and pH 5.4 in the backbone assignment. However, using the visualization of the matching results, it was straightforward to interactively assign these two remaining 4D peaks to His 68 (see Supplementary Material). TM1290 and ubiquitin lack a Trp residue and without changing the experimental conditions, specifically the transfer delays, the 4D APSY-HBCB(CG)CDHD was measured with GB1. This experiment confirmed that the Trp resonances can be correlated and connected to the backbone assignment (see Supplementary Material).

The sequence-specific assignments obtained with the new 4D APSY-HBCB(CG)CDHD can be complemented with a 4D APSY-HCCH-TOCSY or a 4D APSY-HCCH-COSY experiment. The 4D APSY-HCCH-COSY sequence has been published for aliphatic residues (Hiller et al. 2008a)—it can also be used to assign aromatic resonances (Ranjan et al. 2011). The 4D APSY-HCCH-TOCSY pulse sequence is presented in the Supplementary Material (Fig. S3); this experiment also allows correlating CH-groups in His and Trp which are separated by nitrogen nuclei. Both experiments result in 4D HCCH peak lists, which can be connected to the previous assignment via the $^{1}H^{\delta}$ and $^{13}C^{\delta}$ chemical shift values. In the TOCSY version the mixing time can be varied in different APSY projections (Hiller et al. 2008a) leading to intensity changes in the set of projections that allow to discriminate between ε and ζ resonances in Phe and Tyr, and between ε_3, ζ_2, ζ_3 and η_2 resonances for Trp.

The 4D APSY-HBCB(CG)CDHD experiment allows very efficient assignment, but has similar limitations in sensitivity as the corresponding conventional experiments (Yamazaki et al. 1993; Löhr et al. 2002, 2005, 2007). Chemical shift anisotropy (CSA) and strong proton dipolar relaxation as well as the compromises required to include simultaneously all aromatic amino acid types in one experiment limit the sensitivity. As for many multi-dimensional experiments, the recording of every additional indirect dimension reduces the S/N by a factor of $\sqrt{2}$ also in projection spectroscopy (Hiller et al. 2005) due to quadrature detection. Note however that for the projection spectra used in APSY experiments, this factor of $\sqrt{2}$ applies only for those evolution times that are actually included in a given projection. Thus, by a suitable choice of the projection angle set it is possible to circumvent the accumulation of these sensitivity reduction factors and to record a high-dimensional APSY experiment with the relative sensitivity of a low-dimensional experiment (Hiller et al. 2008b). The APSY experiments are recorded as a set of projections. Statistical effects partially compensate for low sensitivity, since cross peaks close to the noise level can reliably be identified (Fig. 3). Furthermore, the high dimensionality of the experiment reduces signal overlap. Since the resulting peak list provides both for the aromatic ring and for the backbone two dimensions for matching, the new experiment provides a powerful tool to unambiguously link and assign aromatic carbon and proton signals to the protein backbone assignment. These findings are confirmed by independent, successful applications of the new method (Ranjan et al. 2011).

As an alternative to the proposed set of experiments, different versions of a 4D APSY-HBCB(CG)CC-TOCSY-H^{aro} experiments based on a published pulse sequence (Löhr et al. 2007) were analyzed. These experiments correlate the backbone resonances with most of the aromatic side chain signals in one experiment. However, the signal losses due to the compromises necessary to include all aromatic amino acids in one experiment were much more pronounced, the experimental sensitivity was therefore significantly reduced in comparison with the 4D APSY-HBCB(CG)CDHD experiment. Thus, the use of the 4D APSY-HBCB(CG)CDHD experiment, optionally in connection with a 4D APSY-HCCH COSY or TOCSY experiment, may lead to more comprehensive results.

Conclusions

The 4D APSY-HBCB(CG)CDHD experiment was successfully applied with three proteins, and led to 4D chemical shift correlations for all four aromatic amino acid types. All obtained 4D peaks could be matched to the existing backbone assignments, and therewith sequence-specifically assigned. The automation of the matching procedure was only impeded by incomplete backbone assignment data, or differences in the sample conditions. In the latter cases, the described interactive approach still provided an efficient assignment of the 4D APSY-HBCB(CG)CDHD peak list. Based on our experimental results we expect an application range for folded proteins up to 20 kDa, depending on the experimental conditions. Further, the experiment seems very well suited for NMR studies of intrinsically unfolded and denatured proteins.

Acknowledgments We thank Prof. Kurt Wüthrich for the provision of TM1290, and Dr. Daniel Burschowsky for support with the expression of ubiquitin. The Swiss National Fund (SNF) is gratefully acknowledged for financial support (projects 200021_120048 and 3100A0-113730).

References

Bax A, Clore GM, Gronenborn AM (1990) ^{1}H–^{1}H correlation via isotropic mixing of ^{13}C magnetization, a new 3-dimensional

approach for assigning ^{1}H and ^{13}C spectra of ^{13}C-enriched proteins. J Magn Reson 88(2):425–431

Billeter M, Braun W, Wüthrich K (1982) Sequential resonance assignments in protein ^{1}H NMR spectra—computation of sterically allowed proton–proton distances and statistical analysis of proton–proton distances in single-crystal protein conformations. J Mol Biol 155(3):321–346

Burschowsky D, Rudolf F, Rabut G, Herrmann T, Matthias P, Wider G (2011) Structural analysis of the conserved ubiquitin-binding motifs (UBMs) of the translesion polymerase iota in complex with ubiquitin. J Biol Chem 286(2):1364–1373

Carlomagno T, Maurer M, Sattler M, Schwendinger MG, Glaser SJ, Griesinger C (1996) PLUSH TACSY: Homonuclear planar TACSY with two-band selective shaped pulses applied to Cα, C$'$ transfer and Cβ, C-aromatic correlations. J Biomol NMR 8(2): 161–170

Cornilescu G, Marquardt JL, Ottiger M, Bax A (1998) Validation of protein structure from anisotropic carbonyl chemical shifts in a dilute liquid crystalline phase. J Am Chem Soc 120(27):6836–6837

Emsley L, Bodenhausen G (1990) Gaussian pulse cascades—new analytical functions for rectangular selective inversion and in-phase excitation in NMR. Chem Phys Lett 165(6):469–476

Etezady-Esfarjani T, Peti W, Wüthrich K (2003) NMR assignment of the conserved hypothetical protein TM1290 of *Thermotoga maritima*. J Biomol NMR 25(2):167–168

Etezady-Esfarjani T, Herrmann T, Peti W, Klock HE, Lesley SA, Wüthrich K (2004) Letter to the Editor: NMR structure determination of the hypothetical protein TM1290 from *Thermotoga maritima* using automated NOESY analysis. J Biomol NMR 29(3): 403–406

Fiorito F, Hiller S, Wider G, Wüthrich K (2006) Automated resonance assignment of proteins: 6D APSY-NMR. J Biomol NMR 35(1): 27–37

Früh DP, Arthanari H, Wagner G (2005) Unambiguous assignment of NMR protein backbone signals with a time-shared triple-resonance experiment. J Biomol NMR 33(3):187–196

Gossert AD, Hiller S, Fiorito F, Wüthrich K (2007) NMR assignment of the *E. coli* type 1 pilus protein FimF. J Biomol NMR 38(2):195

Gossert AD, Hiller S, Fernandez C (2011) Automated NMR resonance assignment of large proteins for protein-ligand interaction studies. J Am Chem Soc 133(2):210–213

Grzesiek S, Bax A (1993) Amino-acid type determination in the sequential assignment procedure of uniformly ^{13}C/^{15}N-enriched proteins. J Biomol NMR 3(2):185–204

Grzesiek S, Bax A (1995) Audio-frequency NMR in a nutating frame—application to the assignment of phenylalanine residues in isotopically enriched proteins. J Am Chem Soc 117(24): 6527–6531

Güntert P, Dötsch V, Wider G, Wüthrich K (1992) Processing of multidimensional NMR data with the new software PROSA. J Biomol NMR 2(6):619–629

Hiller S, Fiorito F, Wüthrich K, Wider G (2005) Automated projection spectroscopy (APSY). Proc Natl Acad Sci USA 102(31):10876–10881

Hiller S, Wasmer C, Wider G, Wüthrich K (2007) Sequence-specific resonance assignment of soluble nonglobular proteins by 7D APSY-NMR Spectroscopy. J Am Chem Soc 129(35):10823–10828

Hiller S, Joss R, Wider G (2008a) Automated NMR assignment of protein side chain resonances using automated projection spectroscopy (APSY). J Am Chem Soc 130(36):12073–12079

Hiller S, Wider G, Wüthrich K (2008b) APSY-NMR with proteins: practical aspects and backbone assignment. J Biomol NMR 42(3): 179–195

Kupce E, Freeman R (2003) Projection-reconstruction of three-dimensional NMR spectra. J Am Chem Soc 125(46): 13958–13959

Logan TM, Olejniczak ET, Xu RX, Fesik SW (1993) A general method for assigning NMR spectra of denatured proteins using 3D HC(CO)NH-TOCSY triple resonance experiments. J Biomol NMR 3(2):225–231

Löhr F, Katsemi V, Betz M, Hartleib J, Rüterjans H (2002) Sequence-specific assignment of histidine and tryptophan ring ^{1}H, ^{13}C and ^{15}N resonances in ^{13}C/^{15}N- and ^{2}H/^{13}C/^{15}N-labelled proteins. J Biomol NMR 22(2):153–164

Löhr F, Rogov VV, Shi MC, Bernhard F, Dötsch V (2005) Triple-resonance methods for complete resonance assignment of aromatic protons and directly bound heteronuclei in histidine and tryptophan residues. J Biomol NMR 32(4):309–328

Löhr F, Hänsel R, Rogov VV, Dötsch V (2007) Improved pulse sequences for sequence specific assignment of aromatic proton resonances in proteins. J Biomol NMR 37(3):205–224

Marion D, Ikura M, Tschudin R, Bax A (1989) Rapid recording of 2D NMR-spectra without phase cycling—application to the study of hydrogen-exchange in proteins. J Magn Reson 85(2):393–399

Morris GA, Freeman R (1979) Enhancement of NMR signals by polarization transfer. J Am Chem Soc 101(3):760–762

Ranjan N, Damberger FF, Sutter M, Allain FHT, Weber-Ban E (2011) Solution structure and activation mechanism of ubiquitin-like small archaeal modifier proteins. J Mol Biol 405(4):1040–1055

Sachs DH, Schechter AN, Cohen JS (1971) NMR titration curves of histidine ring protons.1. Influence of neighboring charged groups. J Biol Chem 246(21):6576–6580

Shaka AJ, Keeler J, Frenkiel T, Freeman R (1983) An improved sequence for broad-band decoupling—WALTZ-16. J Magn Reson 52(2):335–338

Szyperski T, Wider G, Bushweller JH, Wüthrich K (1993) Reduced dimensionality in triple-resonance NMR experiments. J Am Chem Soc 115(20):9307–9308

Szyperski T, Yeh DC, Sukumaran DK, Moseley HNB, Montelione GT (2002) Reduced-dimensionality NMR spectroscopy for high-throughput protein resonance assignment. Proc Natl Acad Sci USA 99(12):8009–8014

Takeuchi K, Früh DP, Sun Z-YJ, Hiller S, Wagner G (2010) CACA-TOCSY with alternate ^{13}C–^{12}C labeling: a ^{13}C$^{\alpha}$ direct detection experiment for mainchain resonance assignment, dihedral angle information, and amino acid type identification. J Biomol NMR 47(1):55–63

Torizawa T, Ono AM, Terauchi T, Kainosho M (2005) NMR assignment methods for the aromatic ring resonances of phenylalanine and tyrosine residues in proteins. J Am Chem Soc 127(36): 12620–12626

Wagner G, Wüthrich K (1982) Sequential resonance assignments in protein ^{1}H NMR spectra—basic pancreatic trypsin-inhibitor. J Mol Biol 155(3):347–366

Wider G, Dreier L (2006) Measuring protein concentrations by NMR spectroscopy. J Am Chem Soc 128(8):2571–2576

Yamazaki T, Forman-Kay JD, Kay LE (1993) 2-dimensional NMR experiments for correlating ^{13}C$^{\beta}$ and ^{1}H$^{\delta/\varepsilon}$ chemical shifts of aromatic residues in ^{13}C-labeled proteins via scalar couplings. J Am Chem Soc 115(23):11054–11055

Zerbe O, Szyperski T, Ottiger M, Wüthrich K (1996) Three-dimensional ^{1}H-TOCSY-relayed ct- ^{13}C, ^{1}H-HMQC for aromatic spin system identification in uniformly ^{13}C-labeled proteins. J Biomol NMR 7(2):99–106